2017

Determination and Validation of High-Pressure Equilibrium Adsorption Isotherms via a Volumetric System

Hind Jihad Kadhim Shabbani
University of South Carolina

DETERMINATION AND VALIDATION OF HIGH-PRESSURE EQUILIBRIUM ADSORPTION ISOTHERMS VIA A VOLUMETRIC SYSTEM

By

Hind Jihad Kadhim Shabbani

Bachelor of Science
Al-Qadisiya University, 2013

Submitted in Partial Fulfilment of the Requirements

For the Degree of Master of Science in

Chemical Engineering

College of Engineering and Computing

University of South Carolina

2017

Accepted by:

James A. Ritter, Director of Thesis

Armin Ebner, Reader

Jamil Khan, Reader

John Weidner, Reader

Cheryl L Addy, Vice Provost and Dean of the Graduate School

ACKNOWLEDGEMENTS

"Let gratitude be the pillow upon which you kneel to say your nightly prayer

- Dr Maya Angelou

First and foremost I acknowledge first the Higher Committee of Education in Iraq (HCED) that gave me the chance to pursue my degree and offer me sponsorship throughout the way. Secondly, I would like to express my gratitude to Dr James Ritter for accepting me as one of his students and giving me the opportunity to work with him. Special acknowledgement to Dr Ebner Armin who took upon himself to be a true guidance and amazing teacher, his patience and understanding will always be acknowledged. I would also like to acknowledge the efforts of Dr Nicholson Marjorie who gave time and effort in helping me in my research.

Thanks to my two amazing children who gave me hope and happiness through the hardest times. A full-hearted acknowledgement to the two men who believed in me since the beginning, my husband and my father. Thank you for your faith and encouragement, it helped me to be a better student and a better person. My mother, sisters and brothers I appreciate all your prayers and support.

Finally, to all who ever supported me with a kind word or simply by a smile, I'd like to express my gratitude to you for being a part of this journey.

ABSTRACT

Adsorption equilibrium isotherms for N_2, CO_2, and CH_4 on zeolite 13X were investigated at three different temperatures (25.5, 50.5 and 75.5˚C) and a pressure range of (0-6.89475) MPa for CH_4 and N_2 and in the range of (0-4.82633) MPa for CO_2 using built in volumetric apparatus. The results were validated using with a volumetric system (ASAP) at the same temperatures and a pressure up to (160-110) KPa respectively. The experimental results were correlated using three process Langmuir (TPLM). The correlated isotherms were then used to calculate the isosteric heat of adsorption for the three gases on 13X. The resulting data have been used to validate the measurements of these systems and are available in the literature for comparison of zeolite 13X isotherms with newly developed adsorbents.

TABLE OF CONTENTS

LIST OF TABLES

LIST OF FIGURES

CHAPTER 1

INTRODUCTION

The slow but steady decline, despite continuous drilling of natural gas that is considered both cheap and clean source of energy, have put the unconventional sources of natural gas especially shale gas in center-stage. Shale gas and the unconventional sources of natural gas have risen in recent years due to the economic feasibility of extracting these unconventional sources which helped in transforming the energy sector in the United States. Shale gas has been produced on a large scale, almost half the United States supply of natural gas and is expected to make up 14% of the world energy by 2035 according to the international energy agency (IEA). Shale gas which is usually found in low porosity organic shale rocks is being produced by performing hydraulic fracturing and horizontal drilling. Shale gas is mainly composed of methane and small fractions of C2, C3, CO_2, N_2, and a trace amount of other material such as H_2S (refer to Table 1.1, 1.2, 1.3 and 1.4). Fracking fluid is pumped into the well under high pressures which could be ranging from 3.44 MPa up to 85 MPa [1] [2] [3] [4] [5] [6]. After the fracking process is finished, the produced shale gas needs to be sequestered and purified for future use.

High-pressure adsorption attracts research in recent years due to the rise in the production of natural gas that results from unconventional sources such as shale gas. Adsorption isotherms can be measured experimentally using different techniques, but

usually, the most common methods are volumetric and gravimetric. Volumetric method is usually preferable in the laboratory due to its simplicity and low cost [7].

The separation and purification of a gas stream based on a selective adsorption on a solid adsorbent material to produce a gas stream enriched with the less likely adsorbed gas have been used widely in industrial applications [8][9][10]. Adsorption processes such as pressure swing adsorption (PSA) and temperature swing adsorption (TSA) have gained an increased interest in the past years in purification and separation processes. The increased used of these processes is mainly due to low energy required and low capital cost [10]. The most important criteria for choosing an adsorbent for PSA is its adsorption working capacity and selectivity at the conditions required. The most common adsorbents are activated carbon and zeolite due to their large internal surface and complicated pore system [11]. Activated carbon is the most prevalent adsorbent used in separation and purification processes as consequence of its low cost and large surface area [12] [13]. Zeolite, on the other hand, is a crystalline porous aluminosilicate that is being used in the separation processes greatly due to its well-defined structure, surface basicity, the electric field caused by exchangeable cations that are present in its framework, 3D pores and well-defined diameter [8] [14] [15]. It was found that zeolite 13X (NaX) is one of the best types of zeolite in the adsorption process due to its stability, higher capacity and rapid mass transfer [15].

The development of PSA process design and simulation requires the knowledge of the adsorption equilibrium data such as adsorption isotherms and the isosteric heat of adsorption on a broad range of temperatures and pressures [12] [16]. Adsorption isotherms represent the amount adsorbed (moles of adsorbate/gm of adsorbent) versus pressure at

constant temperature. The availability of isotherms data will help determine the critical dimensions and operation time for adsorption processes design. The adsorption isotherms could be of different shapes reflecting the type of the adsorbate-adsorbent interaction [17] [8]. High-pressure adsorption isotherms are of particular importance considering that it could be used for the separation, purification, and storage of the shale gas.

There have been many studies in the literature on high-pressure adsorption. The adsorption equilibria of CO_2, CO, N_2, CH_4, Ar and H2 were measured on pelletized 13X up to 1 MPa by Park et al [18] using volumetric technique for the temperatures (20, 35 and 50)℃, the isosteric heat of adsorption was also measured from collating experimental results using Langmuir and sips model. High-pressure adsorption isotherms on zeolite 13X were also reported in the literature. The adsorption equilibria of CH_4, N_2 and CO_2, were measured on 13X using the gravimetric technique at a three different temperatures (25, 35 and 50)℃ and in a pressure range of (0-5) MPa by Cavenati et al. [19]. Their results showed that the adsorption capacity of CO_2 on 13X is much higher than the other gases and that 13X could be used for natural gas purification or carbon dioxide capture [19]. High pressure adsorption of CO_2 on 13X using PSA was also investigated by Takamura et al. [20].

In this work, the pure adsorption isotherms of different gases (CH_4, N_2 and CO_2) were measured using the volumetric technique on and zeolite 13X at three temperatures (25.5, 50.5 and 75.5)℃ and in the pressure range of (0-6.895) MPa. The results obtained on 13X were validated by comparison to the ones obtained by ASAP volumetric systems. The heat of adsorption was also calculated for the three gases on13X zeolite using three process Langmuir model (TPLM) These results can be considered as a reference data for

future researches, help in the evaluation of the adsorption capacity of recently developed adsorbents and they could also help with the design of adsorption processes that contain the studied gases under the studied conditions.

Tables (1.1, 1.2, 1.3 and 1.4) show the different possible composition for shale gas for different areas and different sources.

Table 1. 1: composition values for Gas produced from Antrim Shale wells, USA (mol. %) [21].

Well, state	C1	C2	C3	CO_2	N_2
Northern margin Michigan	77.34-96.75	0-3.96	0-0.92	0.01-5.75	0.28-14.33
Western margin, Michigan	60.37-92.48	0.06-6.64	0.07-2.63	3.42-7.47	0.10-28.84
Central Basin , Michigan	57.80-81.16	4.94-11.92	1.87-4.90	0.04-0.17	0.51-36.19
Southern margin, Indiana	27.18-85.37	3.45-4.29	0.4-1	2.97-8.92	0.72-64.27
Southern margin, Ohio	62.24-73.17	0.07-4.76	0.25	0.17-4.46	28.00
Southern margin, Michigan	45.46	5.78	1.8	2.89	43.52
Eastern margin , Michigan	84.62	6.13	1.65	1.22	6.03

Table 1. 2: Natural gas geothermal characteristic compassion from Jiaoshilba, China, shale gas field [22].

C1	C2	C3	CO_2	N_2
95.52-98.95	0.32-0.73	0.01-0.05	0.02-1.07	0.32-2.95

Table 1. 3: Molecular composition of Chestnut park and Clarington seep gases, USA, (vol. %) [23].

sample	C1	C2	C3	iC4	nC4	iC5	C6+	CO_2	N_2	He	H_2	C1
Chestnut	59.75	23.48	11.69	0.810	2.059	0.214	0.120	1.553	0.244	0.005	0.058	59.75
Clarington	87.75	8.50	2.15	0.277	0.400	0.090	0.056	0.07	4.91	0.075	0.262	87.75

Table 1. 4: Longmaxi shale gas main component molecular composition (%) in southern Sichuan Basin, China [24].

C1	C2	C3	CO_2	N_2
97.64-99.59	0.23-0.68	0-0.03	0.01-1.148	0.01-2.95

CHAPTER 2

EXPERIMENTAL

Materials

The zeolite 13X was supplied by Grace Davison (grade 544, 8x12 mesh size). Helium, Nitrogen and methane were provided from PRAXAIR with a purity of 99.999, 99.999 and 99.97% respectively, while carbon dioxide was provided from Airgas with a purity of 99.99%

Experimental Setup

Figure 2.1 shows a schematic of the volumetric setup used in this work. It consisted of two volumetric cells: an antechamber of known volume (9) and a sample chamber (12) separated by both a needle (10) and a ball valve (11). The needle valve is used to regulate the flow between the two cells and the ball valve to isolate the cells from each other during isotherm determination. Additional needle and ball valve pairs are also placed upstream the antechamber (5 and 8) and downstream the sample chamber (13 and 14). The first pair (i.e., valves 5 and 8) is used to regulate the flow into the antechamber and allow or not gas into the antechamber during isotherm determination. The second pair (i.e., valves 13 and 14) are used to regulate and allow the flow leaving the sample chamber during regeneration of the sample via gas purge, which is a step that is explained in more detailed later. The pressure within these cells is measured by using three MKS pressure transducers (19, 20 and 21) that read up to 1000, 250 and 30 Psia, respectively. Two ball valves (17 and 18)

were used to protect the lower pressure transducers 20 and 21, respectively, when operating at pressures that were higher than the maximum recommended values for each one of them. A 15-micron filter (16) is used to protect the transducer from sample dust that may be coming from the sample chamber. The temperature of the sample in the sample chamber is measured by a K type thermocouple (15). A Pfeiffer (TSU 071 E) vacuum pump (7) able to achieve a vacuum up to $5.4x10^{-5}$ mbar is attached upstream needle valve 6 is used for both sample regeneration (also as explained later). A three-way valve (4) is connected between the system and the vacuum pump with the common exit attached to the system so that the system is depressurized via venting of via evacuation through the pump. Feed gassed are admitted into the system through ball valve 1. A three-way valve (2) with the common exit connected toward the feed is used to vent the lines prior to any run. The two volumetric cells, valves 8, 10, 11 13, and 14, and the filter 16 are all placed within a THERMOTRON temperature chamber to keep the temperature of the system controlled at a constant valve during the isotherm determination. All tubing lines used within the chamber were $1/16^{th}$ inch OD. The figure does not show band heaters and glass wool insulation that are temporarily put around the sample chamber for regeneration. These band heater and insulation are removed during isotherm determination or any run that is carried out at lower temperatures.

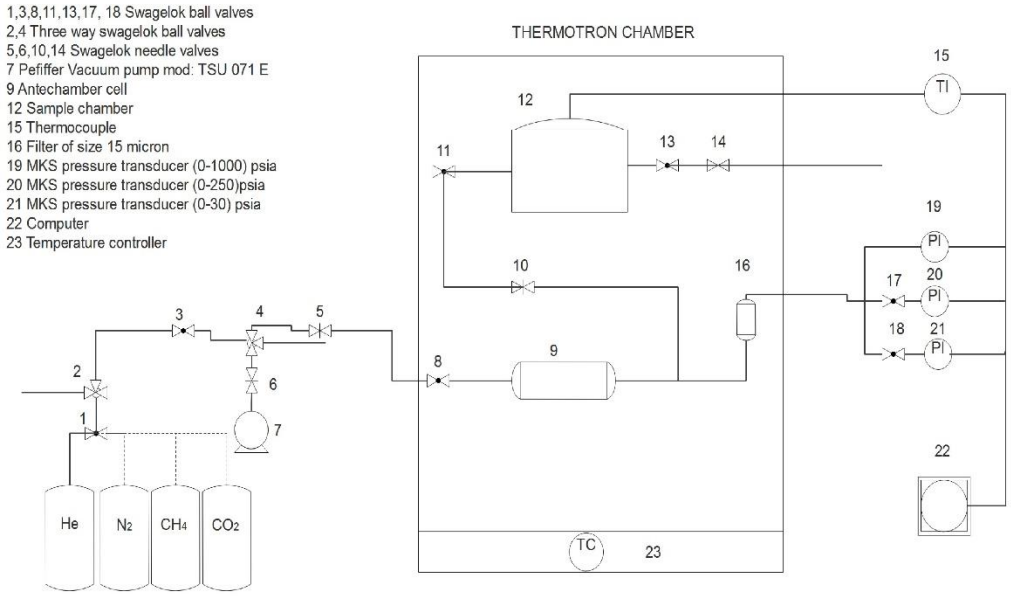

Figure 2. 1: detailed schematic for the volumetric setup.

Sample Chamber

The sample chamber is described in figure (2.2) with detailed schematic (a) and picture of the actual cell and parts involved (b). The chamber consisted of an upper flange (11) containing a k-type thermocouple (2) previously described, a lower flange weld to the sample holding bed (6), a cylindrical sample holder (7) and a mesh holder (4) both made of aluminum, the mesh (10) is used to keep samples that consist of fine powders confined within the chamber cell, and a copper gasket placed between the flanges to seal the chamber cell from leaking (3). Depending on the sample holder, the sample chamber can contain up to 20 g of sample (5). Eight bolts (1) are used to seal the system by bringing both flanges against each other and squeezing the copper gasket. The tip of the thermocouple is placed within the bulk of the sample as shown. The gas access (8) and exit (9) to and from the sample chamber is done through sample holding bed wall. The corresponding gas lines are

connected to the sample chamber via 1/16th vcr fittings. Within the sample chamber, the gas moves upward and downward through the space between the sample holder and the inner wall of the sample chamber before and after it reaches the sample, respectively.

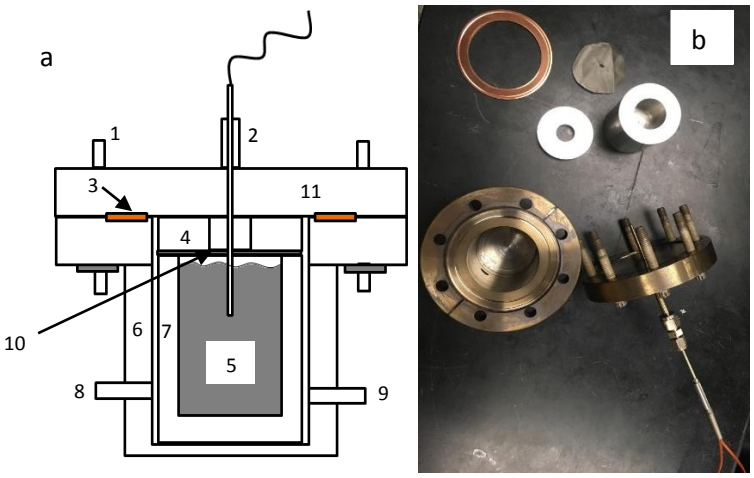

Figure 2. 2: a) Schematic of sample chamber and b) actual components of the sample chamber.

Volume Determination of System Elements

The volumes of the antechamber V^{ac}, empty sample chamber V^{s} (i.e., without sample, mesh, mesh holder and sample holders), sample and mesh holder together V^{h}, and the skeletal volume of the sample V^{a} are determined in different runs with helium and with the aid of steel spheres of known volume V^{sph}. The following four runs are carried out. A first run with the sample chamber being empty; a second run with the sample chamber containing only the spheres of known value; a third run with the sample chamber containing both sample and mesh holders and mesh but without the sample, and a fourth run with the sample chamber containing both sample and mesh holders, mesh and a regenerated sample. In all these runs the same following three steps are carried out. First, the antechamber and sample chamber must be under complete vacuum. This is done by

evacuating these chambers that were originally under helium by opening valves 8, 11, and the three-way valve 4 connecting the both chambers to the vacuum pump. All other valves remain closed. Then, valve 11 and the three-way valve 4 are closed and valves 1, 3, and 8 are opened (with three-way valve 2 connecting helium to the antechamber) to let helium in to pressurize the antechamber from vacuum to a desired pressure, by closing valve 8 again. The pressure within the antechamber is let equilibrate to an initial pressure P^i. Finally ball valve 11 is opened to connect both antechamber and sample chamber. Thus, helium from the antechamber is expanded into the sample chamber (12), which was originally under vacuum. The pressure of the two connecter chambers is let to equilibrate to a final pressure P^f.

The volumes of the antechamber and empty sample chamber are obtained from the run with sample chamber being empty, for which the initial and final pressures are $P^i_{empty}, and\ P^f_{empty}$, and the run with the sample chamber containing the spheres of known volume V^{sph}, for which the initial and final pressures are $P^i_{sph}, and\ P^f_{sph}$, according to the expressions:

$$V^{ac} = V^{sph} \cdot \left(\frac{1}{\frac{P^f_{empty}}{P^i_{empty}} - \frac{P^f_{sph}}{P^i_{sph}}} \right) \tag{1}$$

$$V^{s} = V^{ac} \cdot \left(\frac{P^f_{empty}}{P^i_{empty}} - 1 \right) \tag{2}$$

The volume used by the sample holder, mesh holder and mesh V^h is then obtained from the pressures $P_h^i, and\ P_h^f$ from the run with sample chamber containing the holders and the mesh without the sample according to:

$$V^h = V^s - V^{ac} \cdot \left(\frac{P_h^f}{P_h^i} - 1\right) \quad (3)$$

Finally, the volume used by the regenerated sample is also obtained from the pressures $P_s^i, and\ P_s^f$ from the run with sample chamber containing all sample, holders and mesh according to:

$$V^a = V^s - V^h - V^{ac} \cdot \left(\frac{P_s^f}{P_s^i} - 1\right) \quad (4)$$

Sample regeneration.

Two types of regeneration were carried out on the zeolite 13X sample depending whether the sample was a new sample or whether the sample was already tested with one gas and required analysis with a different gas. In the first case, the sample is purged through with the helium at a flow of no more than 50 cc/min. This was done by having the three-way valve 2 connecting helium with the antechamber, and then opening valves 1, 3, 8, 11 and 13 while having the rest of the valves closed. Then the sample chamber is brought up to 100 ^oC and kept there for an hour before the temperature is raised again to 350 ^oC to leave the sample chamber at that temperature overnight. As previously indicated a band heater and glass wool insulation was placed around sample chamber during regeneration. Before cooling down, valves 3, and 13 are closed, the three-way valve 4 is adjusted to connect the antechamber with the vacuum pump and the system is let fully evacuate. After

the system cools down, the band heater and glass insulation is removed and the THERMOTRON chamber is set to the desired experimental temperature. In the case of changing the working gas (i.e., adsorbate), the sample is purged through with the new working gas at a flow of no more than 50 cc/min. This was done by having the three-way valve 2 connecting the working gas with the antechamber, and then opening valves 1, 3, 8, 11 and 13 while having the rest of the valves closed. Then sample chamber is the brought up only to 160 ^{o}C this time and kept there overnight. Again, a band heater and glass wool insulation was placed around sample chamber during this time. This is done to remove any traces of the previous working gas in the sample. After purging at 160 ^{o}C for an hour, valves 3, and 13 are then closed, the three-way valve 4 is adjusted to connect the antechamber with the vacuum pump and the system is let fully evacuate. Vacuum regeneration at 160 ^{o}C is then continued overnight. After the system cools down, the band heater and glass insulation is removed and the THERMOTRON chamber is set to the desired experimental temperature.

Isotherm Determination

Isotherms of any of the three tested gasses (N_2, CH_4 and CO_2) were obtained by setting the temperature controller of the THERMOTRON temperature chamber set at the desired temperature. The isotherm determination process was initialized by first having both antechamber and sample chamber under vacuum, with all valves closed except for valves 1 and 3 and the three-way valve 2 that was set to connect the working gas with the line feeding the antechamber through valves 3 and 8 (which is closed). The sample chamber which contains the sample holder, the mesh holder, the mesh and a sample of zeolite 13X of mass m^a that has been previously regenerated. Valve 8 is then opened and the

antechamber is let pressurized till the desired pressure is reached by closing valve 8 again. The antechamber is let equilibrate and initial pressure of this step P_1^i is recorded and the total moles of the working gas into the system is determined based on thee known volume of the antechamber V^{ac} and assuming a real gas equation of state for the working gas. Then ball valve 11 is opened and the gas from the antechamber is expanded into the sample chamber. The connected antechamber and sample chamber are to let to equilibrate for the next 60 min to have the final pressure of the step P_1^f recorded. The latter piece information will help evaluate the first point of the isotherm. Valve 11 is then closed and valve 8 is reopened to start the second step by refilling the antechamber with the working gas to a new desired pressure by closing again valve 8. The antechamber is let equilibrate and the new initial pressure P_2^i of the second step is recorded and then used together with P_1^f to evaluate the new mass of working gas into the system. The valve 11 is reopened and the system is again let to equilibrate for the next 60 min to get both the final pressure of step two P_2^f to evaluate the second point of the isotherm. Valve 11 is closed and the process of opening and closing valve 8 and opening and closing valve 11 repeated up to the desired pressures within the limits of the higher most transducer (i.e, 1000 Psia). Numerically, a point of the isotherm at step j, q_j, in equilibrium at temperature T and final pressure P_j^fthat is determined when both antechamber and sample chamber are connected (valve 11 open and valve 8 closed) is calculated from the following expressions:

$$q_j\left(P_j^f, T\right) = \frac{N_j^a}{m^a} \tag{5}$$

$$\mathrm{N_j^a} = \mathrm{N_j^T} - \mathrm{N_j^g} \tag{6}$$

$$N_j^g = \frac{P_j^f}{RT} \cdot \frac{V^{ex}}{Z\left(P_j^f, T\right)} \quad (7)$$

$$N_j^T = N_{j-1}^T + \Delta N_j \quad (8)$$

$$\Delta N_j = N_j^{ac,i} - N_{j-1}^{ac,f} \quad (9)$$

$$N_j^{ac,i} = \frac{P_j^i}{RT} \cdot \frac{V^{ac}}{Z\left(P_j^i, T\right)} \quad (10)$$

$$N_{j-1}^{ac,f} = \frac{P_{j-1}^f}{RT} \cdot \frac{V^{ac}}{Z\left(P_{j-1}^f, T\right)} \quad (11)$$

With

$$N_0^T = 0 \; and \; P_o = 0 \quad (12)$$

Where $N_j^T, N_j^a and N_j^g$ respectively correspond to the total moles of working gas (both adsorbed and gas phase), the total moles of working gas in adsorbed state and the total moles of working gas in gas state within the system that comprise the antechamber and sample chamber; P_j^i and P_j^f respectively correspond to the equilibrium pressures of the antechamber before and after the gas expansion into the sample chamber through valve 11 ; $N_j^{ac,i}, N_j^{ac,f}$ are the moles of the antechamber before and after the gas expansion into the sample chamber through valve 11, ΔN_j are the new moles of working gas into the system, V^{ex} corresponds to the excluded volume of the system, which is given by:

$$V^{ex} = V^{ac} + V^s - V^h - V^a \quad (13)$$

And Z (P, T) is the compressibility factor, which is calculated from Pitzer Correlations [26]:

$$Z(P,T) = Zo(P,T) + w * Z1(P,T) \quad (14)$$

$$Zo(P,T) = Bo * \left(\frac{Pr}{Tr}\right) \quad (15)$$

$$Z1(P,T) = Bo * \left(\frac{Pr}{Tr}\right) \quad (16)$$

$$Bo = 0.083 - \frac{0.422}{Tr^{1.6}} \quad (17)$$

$$B1 = 0.139 - \frac{0.172}{Tr^{4.2}} \quad (18)$$

$$Pr = \frac{P}{Pc} \quad (19)$$

$$Tr = \frac{T}{Tc} \quad (20)$$

where Pr and Tr is the reduced pressure and temperature, respectably and Tc, Pc and w are the critical temperature, the critical pressure, and acentric factor of the working gas respectively. Refer to table 3.2.

Isotherm Models

Adsorption equilibrium data were correlated using two models for pure gasses to be used in getting the isosteric heat of adsorption Qst of the gas as a function of loading. These two models are the Three Process Langmuir and the Toth equation. Isotherm data obtained elsewhere at lower pressures using an ASAP 2010 volummetric system [28] for the same gasses on the same 13X zeolite from Grace Davison was included in the fitting of these models. All the data from a single gas at all three different temperatures obtained here and elsewhere [28] were regressed using MS excel solver by minimising the following objective function:

$$\sum_{j=1}^{n} \sum_{i=1}^{nj} \left(\log(q_{k,j,i,model}) - \log(q_{k,j,i,experimental})\right)^2 \cdot \Delta P_{k,j,i} \quad (21)$$

Where

$$\Delta P_{k,j,i} = P_{k,j,i} - P_{k,j,i-1} \tag{22}$$

With $P_{k,j,i} > 0 \; for \; i = 1..nj$ and $\Delta P_{k,j,0} = 0$. The subscript k stands for the species, j in expression (21) stands for a given isotherm obtained either here or elsewhere [28], and subscript i stand for a data point of the isotherm. The logarithmic functions are meant to have the best fit within a *log P* vs *log q* plot while the $\Delta P_{k,j,i}$ term in the expression is meant to give more leverage to points that are more spread apart.

The Three Process Langmuir model is an expansion of the Langmuir model, and it describes the adsorption of a gas species on an energetically heterogeneous adsorbent consisting of three homogenous, energetically different sites. The main assumptions of this model are that the adsorbate-adsorbent free energy for each site is constant and the three sites don't interact with each other [25]. The main equation of this model is as follows:

$$q_{k,model} = \sum_{l=1}^{3} \frac{b_{k,l} P_k q_{s,k,l}}{1 + b_{k,l} P_k} \tag{23}$$

where the affinity and saturation values for a site *l* are respectively given by

$$b_{k,l} = b_{k,o,l} exp\left(\frac{B_{k,l}}{T}\right) \tag{24}$$

$$q_{s,k,l} = q_{s,o,k,l} + q_{s,t,k,l} \cdot T \tag{25}$$

Isosteric Heat of Adsorption

The isosteric heat of adsorption is defined as the infinitesimal change of energy of the adsorbate when an infinitesimal change of the amount adsorbed occurs [26]. Heat of adsorption is an essential thermodynamic parameter since it gives an insight into the adsorption mechanism. It is also an important factor in adsorption process design since it

provides information about the heat released or consumed during adsorption or desorption processes respectively [27]. For the Three Process Langmuir used in this work the isosteric heat of adsorption is calculated using the Clausius-Clapeyron for loading explicit type of isotherms:

$$Q_{st,k} = -\frac{RT^2}{P}\left[\frac{\left(\frac{\partial q_{k,model}}{\partial T}\right)_P}{\left(\frac{\partial q_{k,model}}{\partial P}\right)_T}\right] \tag{26}$$

Analytical expressions of the isosteric heat of adsorption for the Three Process Langmuir and Toth models are respectively:

$$Q_{st,k} = R\frac{\sum_{l=1}^{3}\frac{b_{k,l}\left(-b_{k,l}\,P_k\,q_{s,t,k,l}+T\left(B_{k,l}-T\right)+B_{k,l}\,q_{s,o,k,l}\right)}{\left(1+b_{k,l}\,P_k\right)^2}}{\sum_{l=1}^{3}\frac{b_{k,l}\,q_{s,k,l}}{\left(1+b_{k,l}\,P_k\right)^2}} \tag{27}$$

CHAPTER 3

RESULTS AND DISCUSSION

Adsorption isotherms of CO_2, CH_4 and N_2, were measured for 13X for temperatures of (25.5, 50.5 and 75.5)℃ in the pressure range of (0-6.89475) MPa for CH_4 and N_2 and in the range of (0-4.82633) MPa for CO_2. 12.482 g of sample of regenerated 13X was used to determine these isotherms. Table 3.2 shows the thermodynamic data of these gas species at the critical point required for predicting their real gas behavior according to Pitzer's Correlation (Eqs.14 to 20). The volumes of the system and calculated according to procedure described in Eqs (1) through (4) and Eq. (13) are shown in Table 3.1. The Table also includes a calculated skeletal density of the sample of 2.534 g/cm^3, which is consistent with known values for zeolites [30]. Figures (3.1), (3.3), and (3.5) show the adsorption isotherms of N_2, CO_2 and CH_4 respectively on 13X zeolite.

The experimental isotherms for the three gases were correlated using three process Langmuir model and then the correlated isotherms were used to calculate the isosteric heat of adsorption. The equations that are used in three process Langmuir and in the calculation of the heat of adsorption were shown in chapter (2). The fitting parameters can be seen in table (3.10). As can be seen in figures (3.2), (3.4) and (3.6) the plots were additionally plotted in a log- log scale to show the devastations in the low pressure region since under these conditions a small contaminate can lead to a lower equilibrium loading especially for gases with high affinity towards the solid. The points represent the

experimental data while the line represents the TPLM correlated fittings. The TPLM shows good correlation for CH_4 and N_2 on 13X and the results for CO_2 on 13X are good. All the gases isotherms are of type I isotherms according to the IUPAC classification which coincides with the he microporous structure of 13X [29]. The total potential between the adsorbate-adsorbent systems is the sum of the adsorbate-adsorbate potential and the adsorbate-adsorbent potential. The main contributing potential is the adsorbate-adsorbent one. The adsorbate-adsorbent potential is the main contributor, and it is equal to the following;

$$\emptyset = \emptyset D + \emptyset R + \emptyset Ind + \emptyset F\mu + \phi FQ \ldots\ldots \quad (28)$$

In which they represent dispersion, close-range repulsion, induction energy (interaction between the electric field and an induced dipole), the interaction between the electric field and a permanent dipole, interaction between field gradient and a quadrupole moment energy respectively [29]. This explains the adsorption isotherms on 13X in which CO_2 adsorbs more strongly than CH_4 and N_2 due to the higher Polarizability and the dipole moment as can be seen from the table (3.3) and the adsorption capacity on 13X are in the order of CO_2>CH_4>N_2 respectively. Figures (3.1) to (3.6) shows the validation of these results by comparison with volumetric technique, and they showed very good agreement. There are some deviations for CO_2 in the low pressures, and this is contributed to the presence of water because the CO_2 used was of 99.99% purity with 10 ppm of water fraction present and poor regeneration.

Since the isosteric heat of adsorption is an indicator of the adsorbate-adsorbent interaction, it needs to be known. Figure (3.7) to (3.9) shows the isosteric heat of adsorption

on 13X for N_2, CO_2 and CH_4 respectively. The heat of adsorption are in the order of CO_2>N_2>CH_4. The isosteric heat of adsorption for N_2 and CH_4 are constant in 13X. For CO2 the heat of adsorption decreases with increased loadings due to the heterogeneity of the solid surface [28].

The experimental results of the adsorption isotherms were compared to the ones found in the literature and they are in a good agreement with some deviations either at the lower pressures or at the higher pressures and this could be attributed to the different type of sample used in each experiment. Henry's constant was calculated from the following expression:

$$Kh = \sum_{l=1}^{3} b_{k,l}\, q_{s,k,l} \tag{29}$$

Then henry's constant for this experiment and for other ones from the literature were used to calculate Henry's law and plotted against the pressure and compared. The results forum the volumetric setup and park's results [18] are in a very good agreement for the temperatures 25& 50 ◦C for all three gases. While for other experiments there might be some deviations due to the different structure of sample used due to different source. Tables 3.11 To 3.16 Shows the experimental results from the literature and tables 3. 17 Shows the henry's constant for the fitted isotherms. Figures 3.10 To 3. 15 Shows the comparison of the results against what is found in the literature.

Conclusion:

The adsorption isotherms of N_2, CH_4 and CO_2, were measured on 13X zeolite and activated carbon for three different temperatures (25.5, 50.5 and 75.5) ˚C and pressure up to (6.89475) MPa for CH_4 and N_2 and up to (4.82633) MPa for CO_2 using built in volumetric setup. The obtained results were validated against in house volumetric (ASAP)

setup up to pressure (110) KPa. The comparison validates all three systems for 13X with some deviations for activated carbon in the volumetric setup due to either contaminates presence or experimental error due to not performing regeneration after each run in the case of activated carbon. The resulting isotherms were correlated with three process Langmuir model and the correlated isotherms used for the calculation of the isosteric heat of adsorption using Clausius-Clapeyron equation. The correlated isotherms show good matching for methane and nitrogen with acceptable results for carbon dioxide

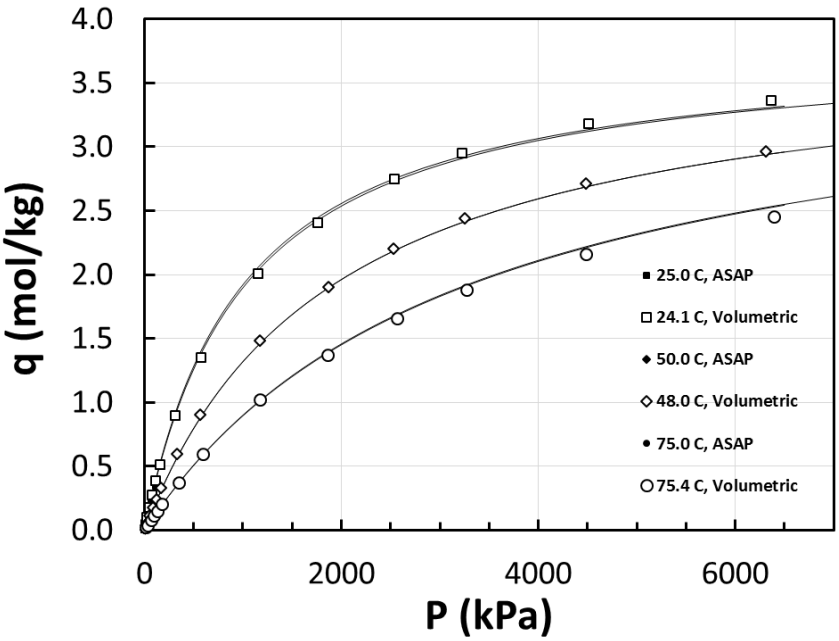

Figure 3. 1: Adsorption equilibrium isotherms of Nitrogen fitted with TPL model at three different temperatures on 13X in rectangular coordinates

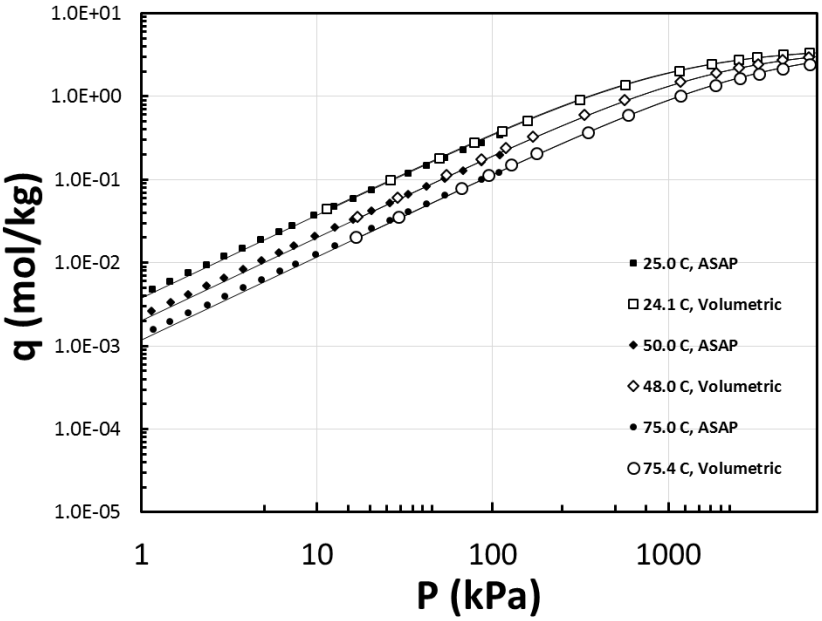

Figure 3. 2: Adsorption equilibrium isotherms of Nitrogen fitted with TPL model at three different temperatures on 13X in logarithmic scale

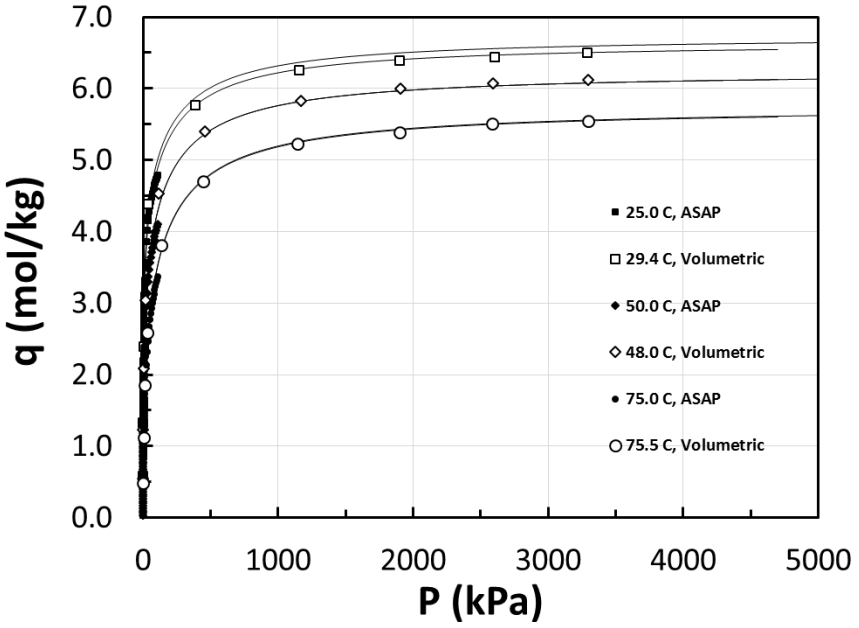

Figure 3. 3: Adsorption equilibrium isotherms of carbon dioxide fitted with TPL model at three different temperatures on 13X in rectangular coordinates

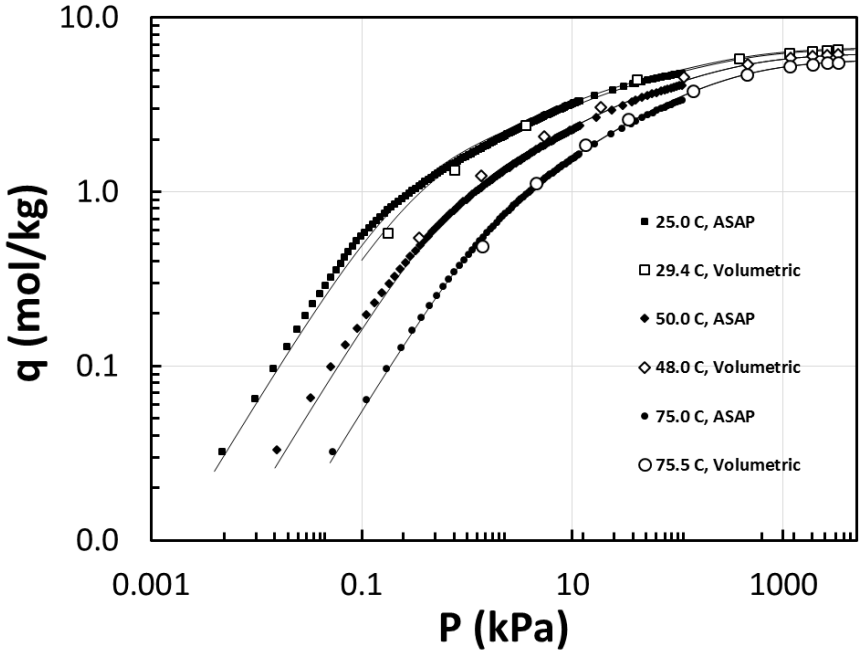

Figure 3. 4: Adsorption equilibrium isotherms of carbon dioxide fitted with TPL model at three different temperatures on 13X in logarithmic scale

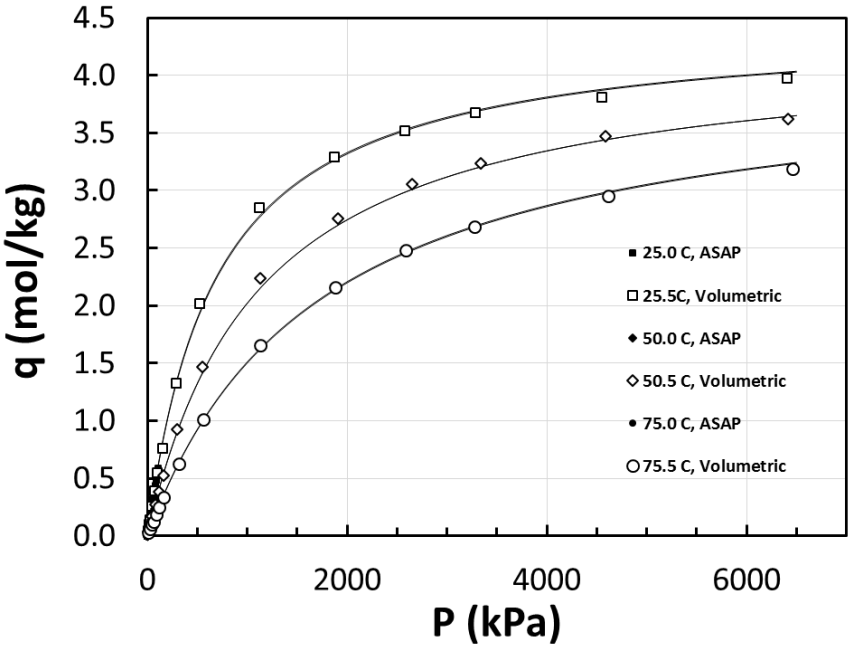

Figure 3. 5: Adsorption equilibrium isotherms of methane fitted with TPL model at three different temperatures on 13X in rectangular coordinates

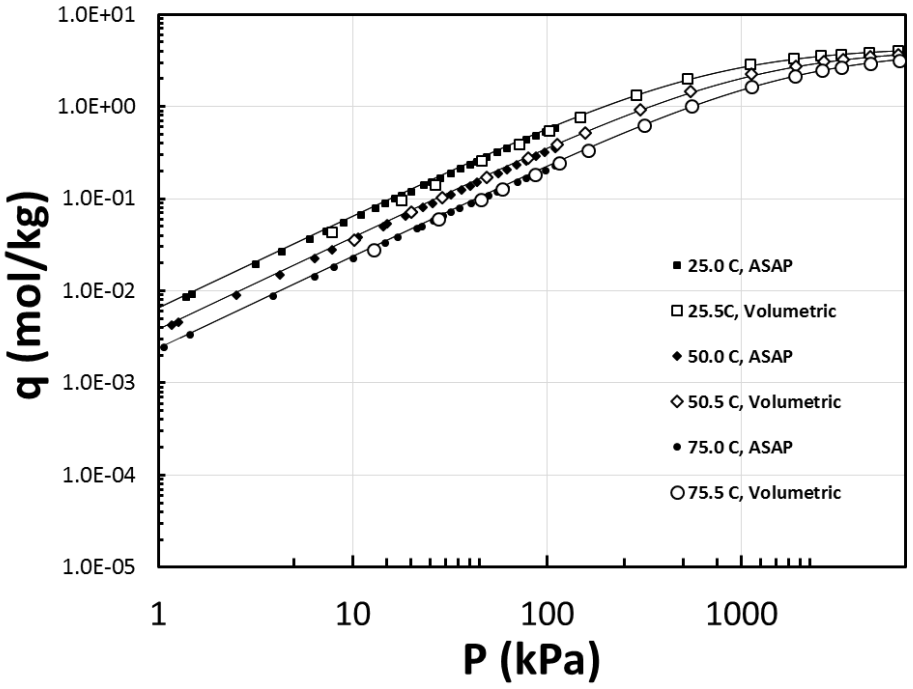

Figure 3. 6: Adsorption equilibrium isotherms of methane fitted with TPL model at three different temperatures on 13X in logarithmic scale

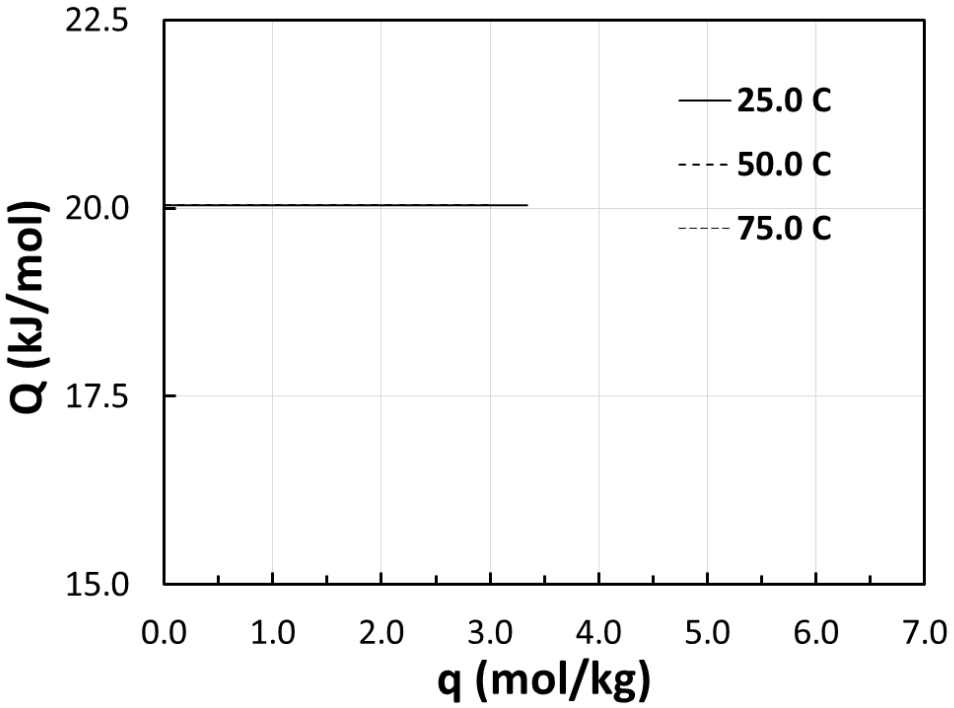

Figure 3. 7: Isosteric heat of adsorption for N2 on 13X with respect to loadings for three different temperatures (Isosteric heat of adsorption equation derived from TPL model)

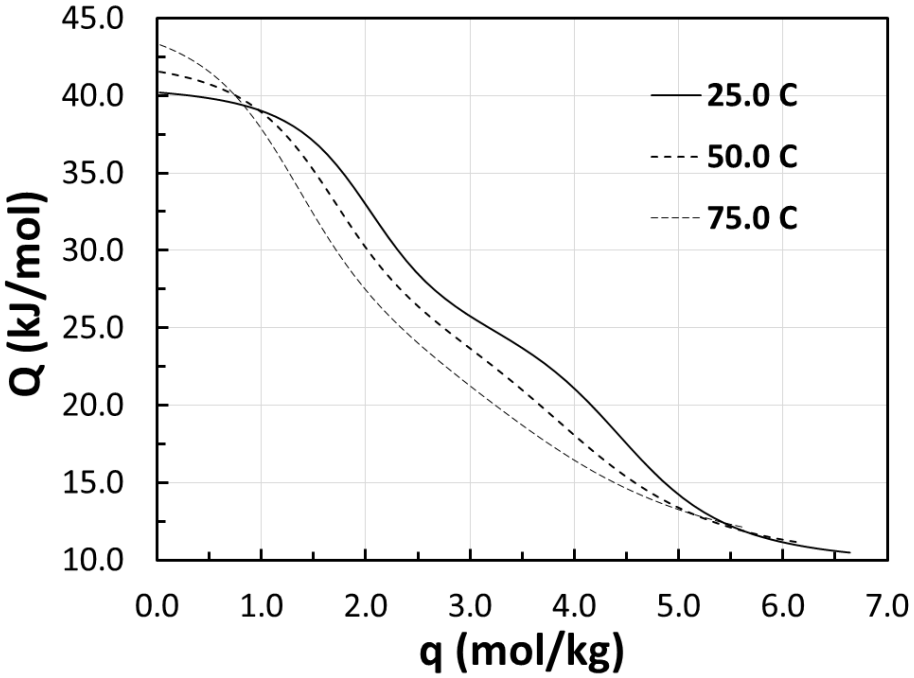

Figure 3. 8: Isosteric heat of adsorption for CO2 on 13X with respect to loadings for three different temperatures (Isosteric heat of adsorption equation derived from TPL model)

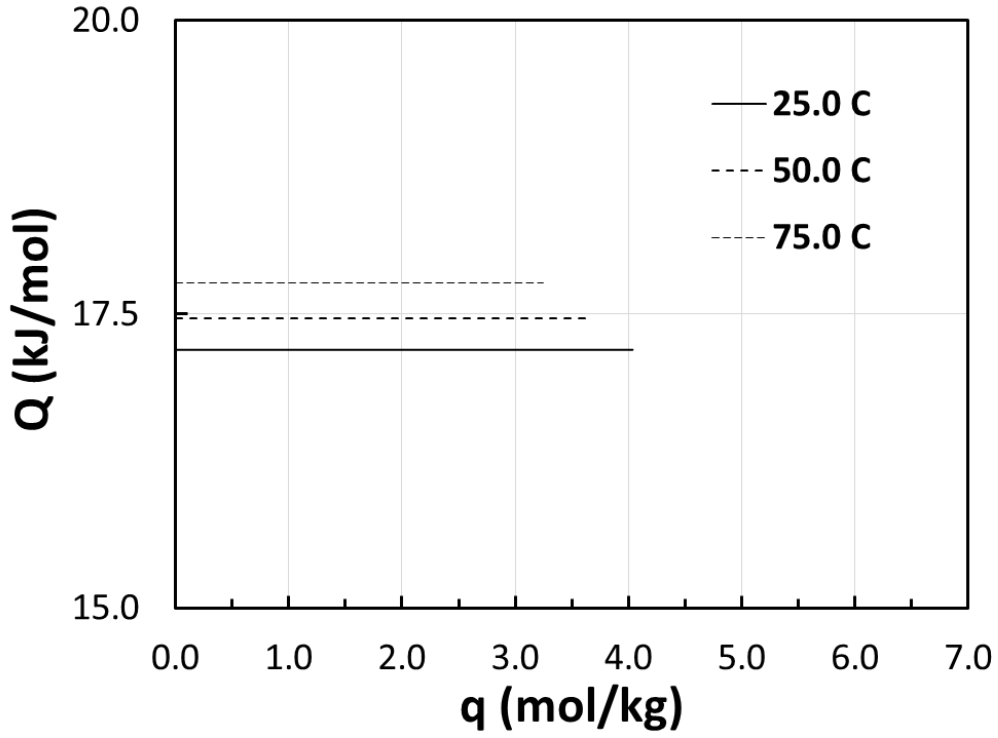

Figure 3. 9: Isosteric heat of adsorption for CH4 on 13X with respect to loadings for three different temperatures (Isosteric heat of adsorption equation derived from TPL model)

Table 3. 1: experimental values of the system different volumes

Volumes, cm^3	
Spheres (V^{sph})	*85.07*
Antechamber (V^{ac})	*168.25*
Empty Sample chamber (V^{s})	*181.82*
Holders and Mesh (V^{h})	*145.09*
Excluded (V^{ex})	*200.06*
Sample Skeletal (V^{a})	*4.93*
Mass of Sample, g	*12.482*
Skeletal Density, g/cm^3	*2.534*

Table 3. 2: Relevant thermodynamic properties of adsorbates [34]

Adsorbate	**Critical temp. [K]**	**Critical pressure [bar]**	**Acentric factor (w)**
N2	126.2	34.00	0.038
CO2	304.2	73.83	0.224
CH4	190.6	45.99	0.012

Table 3. 3: Relevant physical properties of adsorbates [28]

Adsorbate	**Normal BP [K]**	**Kinetic diameter [Å]**	**Polarizability $*10^{25}$ [cm^3]**	**Dipole moment $*10^{18}$ [esu cm]**	**Quadruple moment $*10^{26}$ [esu cm^2]**
N2	77.35	3.64–3.80	17.403	0	1.52
CO2	216.55	3.3	29.11	0	4.3
CH4	111.66	3.758	25.93	0	0

Table 3. 4: Adsorption Equilibrium Isotherm Data of Nitrogen on 13X at 25.5, 50.5, and 75.5 oC measured by volumetric setup

T=25 ºC		T=50 ºC		T=75 ºC	
P	**q**	**P**	**q**	**P**	**q**
(kPa)	**(mol/kg)**	**(kPa)**	**(mol/kg)**	**(kPa)**	**(mol/kg)**
0	0	0	0	0	0
11.41768	0.044129	16.90589	0.035815	16.6232	0.020509
26.33443	0.098003	28.69588	0.060205	29.0613	0.035848
49.93511	0.180516	54.396	0.11281	66.53073	0.079966
78.7413	0.274327	86.32896	0.175306	95.01632	0.113546
113.7734	0.383804	119.6064	0.238189	127.4871	0.149971
158.3548	0.509621	170.0172	0.328564	178.3805	0.206492
315.503	0.895106	332.3606	0.595363	348.3219	0.374158
570.7598	1.354394	563.5893	0.907317	588.8792	0.599696
1157.488	2.007926	1168.368	1.485905	1175.028	1.020976
1762.156	2.404517	1870.541	1.90527	1860.889	1.372789
2536.572	2.751734	2529.126	2.201628	2564.772	1.660218
3229.769	2.950522	3254.038	2.439077	3269.138	1.883661
4510.397	3.182799	4480.06	2.715443	4480.06	2.162836
6362.46	3.365546	6313.852	2.968161	6395.555	2.452011

Table 3. 5: Adsorption Equilibrium Isotherm Data of carbon dioxide on 13X at 25.5, 50.5, and 75.5 oC measured by volumetric setup

T=25 ºC		**T=50 ºC**		**T=75 ºC**	
P	**q**	**P**	**q**	**P**	**q**
(kPa)	**(mol/kg)**	**(kPa)**	**(mol/kg)**	**(kPa)**	**(mol/kg)**
0	0	0	0	0	0
0.179263065	0.579312384	0.351631396	0.540349764	1.389288752	0.489912398
0.761868025	1.332857205	1.365157186	1.234486513	4.478129253	1.121579006
3.602498129	2.38636373	5.346865644	2.085835535	13.35165096	1.859330535
41.3546101	4.387127999	18.54683247	3.036242203	34.0137876	2.593209382
385.3052735	5.763305492	114.4180985	4.526820317	137.8808757	3.814307086
1158.797819	6.253828343	460.3613398	5.400486074	448.2610829	4.707190317
1900.257434	6.384619023	1169.208866	5.827728188	1146.421773	5.231563003
2603.313385	6.439147598	1905.497431	5.993435827	1899.499013	5.38559879
3290.373554	6.495471075	2593.660758	6.075240514	2586.766025	5.508690147
4523.634492	6.240336579	3293.683026	6.120874851	3295.544604	5.541869091

Table 3. 6: Adsorption Equilibrium Isotherm Data of methane on 13X at 25.5, 50.5, and 75.5 oC measured by volumetric setup

T=25 ºC		T=50 ºC		T=75 ºC	
P	**q**	**P**	**q**	**P**	**q**
(kPa)	**(mol/kg)**	**(kPa)**	**(mol/kg)**	**(kPa)**	**(mol/kg)**
0	0	0	0	0	0
7.799322	0.0435	10.15249	0.0358	12.84834	0.0276
17.95664	0.0963	20.12917	0.071	27.63409	0.06
26.82741	0.142	28.77379	0.1014	45.50869	0.0986
46.405	0.2594	48.86297	0.1714	58.66591	0.1269
72.30162	0.3889	79.75448	0.275	86.55993	0.1853
103.5685	0.5471	113.0219	0.3831	116.0066	0.2458
149.3365	0.761	158.2169	0.523	162.1848	0.3377
287.6138	1.3278	302.2996	0.9263	315.5375	0.6297
526.7197	2.0157	549.0828	1.468	556.6463	1.0118
1120.187	2.8505	1129.992	2.2361	1127.123	1.653
1868.473	3.2932	1905.842	2.7542	1884.606	2.1616
2577.458	3.52	2648.819	3.0517	2587.249	2.4824
3280.169	3.6749	3340.36	3.2319	3273.137	2.6833
4555.143	3.8084	4583.757	3.4731	4616.3	2.95
6404.173	3.9761	6414.17	3.6177	6464.847	3.1894

Table 3. 7: Adsorption Equilibrium Isotherm Data of Nitrogen on zeolite 13X at 25, 50, and 75 oC measured by ASAP2010

T=25 ºC		**T=50 ºC**		**T=75 ºC**	
P	**q**	**P**	**q**	**P**	**q**
(kPa)	**(mol/kg)**	**(kPa)**	**(mol/kg)**	**(kPa)**	**(mol/kg)**
0.0916	0.0004	0.1109	0.0002	0.1231	0.0002
0.1453	0.0006	0.1709	0.0004	0.1804	0.0002
0.1673	0.0007	0.2119	0.0005	0.2045	0.0003
0.2087	0.0009	0.2683	0.0006	0.2696	0.0004
0.2653	0.0011	0.3416	0.0008	0.3409	0.0005
0.3412	0.0015	0.4311	0.0010	0.4326	0.0006
0.4303	0.0019	0.5473	0.0013	0.5483	0.0008
0.5464	0.0024	0.7238	0.0017	0.7242	0.0010
0.7222	0.0031	0.9135	0.0021	0.9037	0.0012
0.9057	0.0039	1.1416	0.0026	1.1644	0.0016
1.1509	0.0048	1.4676	0.0034	1.4568	0.0020
1.4528	0.0060	1.8451	0.0042	1.8526	0.0025
1.8400	0.0076	2.3575	0.0053	2.3608	0.0031
2.3354	0.0095	2.9590	0.0066	2.9792	0.0039
2.9642	0.0119	3.7785	0.0083	3.7808	0.0050
3.7668	0.0150	4.8152	0.0105	4.8198	0.0063
4.7976	0.0190	6.1007	0.0133	6.1088	0.0080
6.0928	0.0239	7.3829	0.0159	7.5109	0.0098
7.1756	0.0280	9.7485	0.0208	9.8386	0.0127
9.6284	0.0370	12.5605	0.0265	12.5692	0.0162
12.5480	0.0475	15.9710	0.0333	15.9791	0.0204
15.9635	0.0596	20.3334	0.0420	20.3332	0.0258
20.3150	0.0747	25.9128	0.0529	25.9049	0.0326
25.9110	0.0938	33.0686	0.0666	33.0681	0.0412
33.1279	0.1179	41.8915	0.0831	41.8834	0.0515
41.8928	0.1464	53.3574	0.1039	53.3396	0.0645
53.3523	0.1824	67.8453	0.1296	67.8784	0.0805
67.8942	0.2262	86.5016	0.1611	86.4661	0.1001
86.4757	0.2794	110.0083	0.1990	108.4670	0.1220
110.0391	0.3429				

Table 3. 8: Adsorption Equilibrium Isotherm Data of Carbon Dioxide on zeolite 13X at 25, 50, and 75 oC measured by ASAP2010

T=25 ºC		**T=50 ºC**		**T=75 ºC**	
P	**q**	**P**	**q**	**P**	**q**
(kPa)	**(mol/kg)**	**(kPa)**	**(mol/kg)**	**(kPa)**	**(mol/kg)**
0.0048	0.0324	0.0156	0.0330	0.0527	0.0324
0.0097	0.0648	0.0329	0.0660	0.1110	0.0646
0.0145	0.0972	0.0510	0.0990	0.1719	0.0966
0.0194	0.1296	0.0700	0.1320	0.2349	0.1284
0.0243	0.1619	0.0898	0.1650	0.3011	0.1599
0.0293	0.1943	0.1109	0.1980	0.3689	0.1914
0.0344	0.2267	0.1326	0.2309	0.4407	0.2225
0.0396	0.2591	0.1554	0.2638	0.5130	0.2535
0.0454	0.2914	0.1800	0.2966	0.5917	0.2852
0.0511	0.3237	0.2055	0.3294	0.6691	0.3164
0.0571	0.3561	0.2320	0.3621	0.7518	0.3459
0.0635	0.3884	0.2610	0.3947	0.8393	0.3763
0.0684	0.4218	0.2902	0.4274	0.9275	0.4063
0.0744	0.4550	0.3227	0.4599	1.0202	0.4359
0.0813	0.4883	0.3547	0.4924	1.1149	0.4653
0.0889	0.5214	0.3913	0.5248	1.2155	0.4943
0.0977	0.5545	0.4255	0.5571	1.3183	0.5239
0.1070	0.5876	0.4638	0.5893	1.4261	0.5527
0.1170	0.6207	0.5033	0.6214	1.5399	0.5811
0.1273	0.6537	0.5453	0.6534	1.6558	0.6100
0.1382	0.6868	0.5890	0.6861	1.7768	0.6389
0.1498	0.7198	0.6365	0.7184	1.9035	0.6676
0.1631	0.7528	0.6900	0.7511	2.0318	0.6962
0.1764	0.7857	0.7415	0.7829	2.1710	0.7243
0.1905	0.8187	0.7975	0.8139	2.3090	0.7524
0.2063	0.8516	0.8581	0.8456	2.4536	0.7800
0.2227	0.8845	0.9205	0.8766	2.6075	0.8071
0.2405	0.9173	0.9825	0.9073	2.7505	0.8344
0.2597	0.9501	1.0534	0.9385	2.9134	0.8609
0.2800	0.9829	1.1224	0.9699	3.0824	0.8877
0.3009	1.0156	1.1974	1.0003	3.2412	0.9142
0.3242	1.0483	1.2745	1.0303	3.4180	0.9399
0.3481	1.0809	1.3504	1.0602	3.6266	0.9705
0.3734	1.1135	1.4375	1.0896	3.8113	0.9958
0.3992	1.1461	1.5283	1.1195	3.9942	1.0216
0.4283	1.1785	1.6165	1.1498	4.2304	1.0514
0.4585	1.2109	1.7194	1.1796	4.4647	1.0815

0.4885	1.2432	1.8135	1.2095	4.7256	1.1110
0.5211	1.2754	1.9229	1.2387	4.9776	1.1410
0.5583	1.3074	2.0257	1.2680	5.2464	1.1706
0.5947	1.3401	2.1430	1.2967	5.5285	1.1995
0.6324	1.3726	2.2545	1.3254	5.8164	1.2284
0.6726	1.4047	2.3751	1.3537	6.1048	1.2573
0.7175	1.4364	2.5070	1.3822	6.4184	1.2859
0.7633	1.4683	2.6325	1.4111	6.7428	1.3142
0.8105	1.5002	2.7569	1.4392	7.0770	1.3419
0.8589	1.5313	2.9036	1.4669	7.4231	1.3697
0.9120	1.5628	3.0507	1.4937	7.7648	1.3973
0.9702	1.5943	3.1799	1.5218	8.1095	1.4250
1.0247	1.6260	3.3459	1.5487	8.4685	1.4518
1.0846	1.6566	3.4911	1.5762	8.8372	1.4781
1.1459	1.6877	3.6699	1.6022	9.2143	1.5037
1.2091	1.7190	3.8323	1.6353	9.6086	1.5291
1.2789	1.7500	3.9901	1.6621	10.0080	1.5542
1.3495	1.7800	4.1604	1.6885	10.4033	1.5791
1.4194	1.8106	4.3447	1.7141	10.8035	1.6040
1.4915	1.8413	4.5451	1.7459	11.1979	1.6288
1.5679	1.8719	4.7644	1.7771	11.6097	1.6527
1.6466	1.9023	5.0042	1.8078	16.1868	1.8772
1.7301	1.9325	5.2502	1.8383	23.2955	2.1396
1.8168	1.9624	5.4780	1.8688	29.3804	2.3159
1.9053	1.9921	5.7272	1.8992	35.6513	2.4677
2.0045	2.0213	5.9875	1.9294	39.9332	2.5569
2.0999	2.0505	6.2661	1.9586	45.7361	2.6680
2.1885	2.0808	6.5339	1.9878	51.7093	2.7674
2.2961	2.1097	6.8144	2.0169	57.2804	2.8503
2.3998	2.1392	7.1228	2.0459	63.0426	2.9292
2.5046	2.1689	7.4234	2.0747	68.8524	3.0003
2.6120	2.1977	7.7352	2.1035	74.4870	3.0645
2.7266	2.2267	8.0520	2.1326	80.2880	3.1261
2.8390	2.2552	8.3681	2.1611	86.0551	3.1811
2.9561	2.2831	8.7081	2.1886	91.6805	3.2325
3.0876	2.3111	9.0551	2.2163	97.5305	3.2812
3.2165	2.3393	9.3903	2.2436	103.2040	3.3244
3.3498	2.3664	9.7603	2.2704	108.9044	3.3665
3.4887	2.3946	10.1181	2.2973		
3.6266	2.4223	10.4874	2.3235		
3.7538	2.4504	10.8580	2.3492		
3.9002	2.4785	11.2399	2.3752		
4.0566	2.5055	11.6296	2.3997		

4.2214	2.5317	16.8062	2.6833
4.3618	2.5597	23.5558	2.9493
4.5376	2.5856	29.8428	3.1357
4.6991	2.6124	36.3075	3.2916
4.8574	2.6395	39.8407	3.3642
5.0365	2.6721	45.7664	3.4730
5.2410	2.7044	51.7058	3.5645
5.4249	2.7305	57.1871	3.6422
5.6106	2.7564	63.1726	3.7151
5.8489	2.7868	68.6987	3.7780
6.0922	2.8171	74.6369	3.8364
6.3354	2.8481	80.1899	3.8878
6.5831	2.8786	86.0533	3.9370
6.8428	2.9093	91.7428	3.9804
7.1198	2.9387	97.4465	4.0222
7.4006	2.9680	103.2414	4.0616
7.6903	2.9968	108.9493	4.0977
7.9851	3.0256		
8.2889	3.0549		
8.6027	3.0837		
8.9188	3.1129		
9.2599	3.1410		
9.5989	3.1687		
9.9299	3.1967		
10.2771	3.2240		
10.6331	3.2504		
10.9999	3.2760		
11.3773	3.3017		
11.7653	3.3267		
16.0176	3.5597		
24.0737	3.8579		
30.4939	4.0212		
37.1568	4.1522		
39.6948	4.1955		
45.8897	4.2858		
51.5554	4.3581		
57.3260	4.4231		
63.1019	4.4793		
68.7687	4.5292		
74.5403	4.5761		
80.3140	4.6178		
85.9815	4.6557		
91.7353	4.6922		

97.5139	4.7257
103.2160	4.7559
108.9226	4.7849

Table 3. 9: Adsorption Equilibrium Isotherm Data of Methane on zeolite 13X at 25, 50, and 75 oC measured by ASAP2010

T=25 ºC		**T=50 ºC**		**T=75 ºC**	
P	**q**	**P**	**q**	**P**	**q**
(kPa)	**(mol/kg)**	**(kPa)**	**(mol/kg)**	**(kPa)**	**(mol/kg)**
0.1092	0.0007	0.1229	0.0004	0.1311	0.0003
0.1342	0.0008	0.1449	0.0005	0.1636	0.0004
0.1491	0.0009	0.1681	0.0006	0.1890	0.0004
0.1670	0.0010	0.1882	0.0007	0.2118	0.0005
0.1871	0.0011	0.2106	0.0008	0.2367	0.0005
0.2095	0.0013	0.2360	0.0008	0.2653	0.0006
0.2349	0.0014	0.2642	0.0009	0.2968	0.0007
0.2630	0.0016	0.2962	0.0011	0.3333	0.0008
0.2952	0.0018	0.3321	0.0012	0.3731	0.0008
0.3307	0.0020	0.3720	0.0013	0.4178	0.0009
0.3710	0.0023	0.4173	0.0015	0.4690	0.0011
0.4161	0.0025	0.4681	0.0017	0.5262	0.0012
0.4670	0.0029	0.5252	0.0019	0.5895	0.0013
0.5238	0.0032	0.5887	0.0021	0.6627	0.0015
0.5881	0.0036	0.6612	0.0024	1.0736	0.0024
0.6597	0.0041	1.1706	0.0042	1.4560	0.0033
0.9493	0.0058	1.2770	0.0046	3.8882	0.0088
1.3879	0.0085	2.5245	0.0090	6.3531	0.0143
1.4952	0.0092	4.2219	0.0150	8.0281	0.0181
3.1836	0.0195	6.3721	0.0226	10.1172	0.0227
4.3461	0.0265	7.8149	0.0277	12.6021	0.0282
6.0228	0.0367	10.6957	0.0377	14.7918	0.0330
7.3264	0.0445	14.3100	0.0503	17.0037	0.0379
8.9778	0.0545	15.0565	0.0530	21.3771	0.0474
11.0556	0.0668	18.6541	0.0654	22.6346	0.0501
13.1512	0.0792	20.6135	0.0721	26.1386	0.0577
14.7042	0.0885	23.0470	0.0804	29.3842	0.0647
16.5891	0.0996	25.8030	0.0897	32.2081	0.0708
17.8008	0.1067	28.8264	0.0999	35.6686	0.0781
20.0072	0.1195	31.8902	0.1102	40.5951	0.0883
23.3537	0.1390	36.4132	0.1252	44.5770	0.0965
25.5590	0.1517	40.2844	0.1380	50.1149	0.1079
28.1444	0.1664	43.8642	0.1497	55.6073	0.1192

32.1282	0.1890	50.0169	0.1696	61.8466	0.1320
35.7685	0.2095	56.1835	0.1894	70.8589	0.1498
40.4091	0.2353	62.3585	0.2089	78.3544	0.1646
43.7004	0.2534	69.8877	0.2323	88.5103	0.1842
49.1229	0.2830	78.1286	0.2580	98.1947	0.2026
55.7803	0.3188	88.2120	0.2881	110.4074	0.2253
62.2651	0.3531	97.7898	0.3165		
70.3511	0.3951	110.3014	0.3526		
78.3769	0.4357				
87.7081	0.4822				
98.4283	0.5343				
109.7388	0.5875				

Table 3. 10: Fitting parameters of the Three Process Langmuir model for 13X

Gas	**qso1**	**b_1^o**	**B_1**	**q1t**	**qso2**	**q2t**	**b_2^o**	**B_2**	**qso3**	**q3t**	**b_3^o**	**B_3**
	mol *kg^{-1}	kPa^{-1}	K	mol /(kg* K)	mol *kg^{-1}	mol /(kg* K)	kPa^{-1}	K	mol *kg^{-1}	mol /(kg* K)	kPa^{-1}	K
CH_4	6.588	2.306E-06	1925.9	-0.0071	1.717	5.53E-03	0	1925.9	0.00	2.88E-11	0	0
CO_2	4.377	7.203E-06	2826.2	-0.0066	8.761	-0.0131	1.394E-06	4341.5	2.296	3.27E-09	1.087E-03	444.2
N_2	3.825	3.027E-07	2410.3	0	3.561	2.34E-16	0	1758.53	0	0	0	0

Table 3. 11: Adsorption Equilibrium Isotherm Data of nitrogen on zeolite 13X at 25, 50 ◦C measured by Park [18].

T= 25 ºC		**T= 5ºC**	
KPa P	mol/Kg q	KPa P	mol/Kg q
0.972	0.004	0.888	0.002
7.245	0.028	7.696	0.015
13.6	0.053	14.45	0.028
19.74	0.076	21.18	0.041
26	0.099	27.92	0.054
32.14	0.121	34.49	0.067
38.19	0.143	40.86	0.079

44.14	0.164	47.16	0.091
49.94	0.184	53.37	0.102
55.83	0.204	59.52	0.114
61.87	0.224	65.46	0.124
67.63	0.243	71.46	0.135
73.22	0.261	77.37	0.146
78.86	0.279	83.43	0.156
84.56	0.296	89.2	0.166
89.98	0.313	95.11	0.176
95.36	0.33	99.94	0.187
99.83	0.349	104.8	0.196
104.4	0.362	136.7	0.25
133.8	0.445	168.6	0.3
163.6	0.527	200.8	0.35
193.6	0.602	232.8	0.398
223.8	0.672	265	0.444
254.2	0.74	297.7	0.49
285	0.804	330.3	0.535
316	0.868	362.9	0.576
347	0.928	395.9	0.616
378.2	0.983	428.4	0.655
409.4	1.04	461.1	0.694
441.1	1.09	494.2	0.73
472.9	1.14	527.2	0.766
504.7	1.19	560.2	0.802
536.5	1.23	593.1	0.834
568.6	1.28	626.4	0.867
600.5	1.32	659.7	0.899
632.8	1.36	692.6	0.931
665.2	1.4	725.8	0.961
697.5	1.44	759.3	0.99
730.1	1.47	792.5	1.02
762.7	1.51	825.8	1.05
795.2	1.54	859.4	1.07
827.6	1.58	892.9	1.1
860.4	1.61	926.4	1.13
893.1	1.64	959.8	1.15
925.8	1.67	993.2	1.18
958.7	1.7		
991.4	1.73		
1024	1.75		

Table 3. 12: Adsorption Equilibrium Isotherm Data of Carbon dioxide on zeolite 13X at 25, 50 ◦C measured by Park [18].

T= 25 ºC		**T= 5ºC**	
KPa	mol/Kg	KPa	mol/Kg
P	q	P	q
0.567	0.529	0.203	0.285
0.777	0.787	0.573	0.551
1.015	1.048	1.147	0.811
1.347	1.304	1.986	1.063
1.809	1.558	3.168	1.311
2.465	1.807	4.733	1.55
3.343	2.056	6.718	1.781
4.402	2.299	9.183	2.004
5.701	2.539	12.17	2.219
7.332	2.774	15.7	2.422
9.369	2.999	19.87	2.616
11.95	3.216	24.61	2.794
15.12	3.417	29.93	2.957
19.11	3.607	35.91	3.109
23.9	3.778	42.66	3.25
29.47	3.928	49.88	3.375
35.99	4.064	57.56	3.488
43.23	4.182	65.86	3.591
51.12	4.286	74.42	3.683
59.71	4.378	83.44	3.768
68.49	4.458	91.45	3.838
77.79	4.529	99.92	3.899
87.33	4.592	108.2	3.953
96.57	4.639	135.6	4.097
105.4	4.686	163.1	4.213
133	4.802	192	4.311
165.2	4.905	223.8	4.399
196.7	4.985	254.1	4.474
227.3	5.047	285.3	4.538
258.4	5.106	316.7	4.597
289.9	5.156	348.9	4.648
321.8	5.2	381.1	4.695
353.8	5.24	413.7	4.739
386.3	5.275	446.6	4.776
418.7	5.308	479.6	4.81
451.6	5.338	512.7	4.844

484.2	5.364	546	4.874
517	5.389	579.2	4.902
550	5.411	612.8	4.928
583.2	5.432	646.4	4.954
616.3	5.457	680.2	4.976
649.8	5.474	714.2	4.998
683	5.495	748	5.019
716.5	5.512	781.7	5.038
749.9	5.525	815.7	5.055
783.5	5.538	849.8	5.073
817.1	5.55	884	5.087
850.5	5.561	917.8	5.108
884.3	5.571	952	5.118
918.1	5.582	986.3	5.134
951.9	5.592	1021	5.147
985.4	5.604		
1019	5.613		

Table 3. 13: Adsorption Equilibrium Isotherm Data of Methane on zeolite 13X at 25, 50 ◦C measured by Park [18].

T= 25 ºC		**T= 5ºC**	
KPa P	mol/Kg q	KPa P	mol/Kg q
0.592	0.004	0.829	0.003
5.84	0.039	6.974	0.024
11.25	0.074	13.27	0.045
16.46	0.108	19.38	0.066
21.51	0.14	25.4	0.086
26.73	0.172	31.34	0.106
31.65	0.203	37.43	0.126
36.64	0.233	43.1	0.145
41.34	0.261	48.8	0.163
46.37	0.291	54.47	0.181
51.34	0.32	59.91	0.198
56.08	0.348	65.29	0.215
60.7	0.374	70.84	0.233
65.37	0.4	75.98	0.249
70.1	0.427	81.02	0.264
74.41	0.45	85.93	0.279
79	0.475	90.79	0.294

83.34	0.499	94.74	0.307
87.66	0.522	98.48	0.319
91.98	0.545	102.4	0.332
95.46	0.562	135.3	0.427
98.75	0.58	167.7	0.515
102.2	0.599	199.5	0.597
132.3	0.745	230.6	0.676
162.1	0.881	261.1	0.748
191.6	1.007	291	0.815
221	1.122	321.8	0.883
249.9	1.231	352.8	0.948
278.6	1.328	383.7	1.012
307	1.419	415.1	1.07
334.9	1.504	447.1	1.126
364.4	1.588	478.7	1.179
394.6	1.668	510.4	1.235
424.9	1.744	542.5	1.285
455.7	1.819	574.6	1.335
486.5	1.888	607.1	1.381
517.5	1.953	639.8	1.426
549	2.015	672.2	1.473
580.5	2.077	704.9	1.512
612.2	2.135	737.4	1.551
644	2.19	770.3	1.589
675.9	2.243	803.2	1.625
708.2	2.292	836.3	1.661
740.5	2.344	869.4	1.695
772.8	2.399	902.5	1.727
805.8	2.441	935.7	1.761
838.7	2.484	969.2	1.789
871.6	2.527	1002	1.819
904.5	2.568		
937.7	2.608		
970.8	2.647		
1004	2.695		

Table 3. 14: Adsorption Equilibrium Isotherm Data of nitrogen on zeolite 13X at 25, 50 ◦C measured by Simone Cavenati [19].

T= 25 ºC		**T= 5ºC**	
KPa	mol/Kg	KPa	mol/Kg
P	q	P	q
6.13	0.024	9.03	0.015
11.05	0.038	19.12	0.034
25.11	0.082	40.06	0.074
39.2	0.123	55.11	0.098
50.03	0.156	105	0.187
90.02	0.264	175	0.299
170	0.46	220	0.357
260	0.68	280	0.457
310	0.8	360	0.569
390	0.93	360	0.695
570	1.24	470	0.695
655	1.39	570	0.838
745	1.5	680	0.969
990	1.83	800	1.104
1095	1.976	1000	1.303
1280	2.149	1155	1.443
1585	2.432	1340	1.61
1770	2.592	1680	1.875
1935	2.717	2160	2.201
2205	2.909	2405	2.335
2360	3.011	2620	2.459
2595	3.161	3065	2.704
3170	3.491	3340	2.834
3230	3.528	3490	2.916
3685	3.763	3920	3.106
4010	3.923	4470	3.339
4400	4.084	4720	3.442
4725	4.214		

Table 3. 15: Adsorption Equilibrium Isotherm Data of Carbon dioxide on zeolite 13X at 25, 50 ◦C measured by Simone Cavenati [19].

T= 25 ºC		**T= 5ºC**	
KPa P	mol/Kg q	KPa P	mol/Kg q
1.18	1.147	1.06	0.356
6.1	2.249	2.14	0.529
29.05	3.659	5.01	1.06
86.1	4.5	9.07	1.43
160	5.06	24.23	2.09
310	5.58	42.2	2.49
525	6.04	75.03	2.9
1015	6.52	145	3.4
1445	6.92	270	3.915
1935	6.96	390	4.1
2280	7.09	545	4.329
2660	7.22	705	4.532
3200	7.372	850	4.74
		1010	4.82
		1175	4.93
		1455	5.2
		1720	5.24
		2125	5.43
		2695	5.62
		3395	5.762

Table 3. 16 :Adsorption Equilibrium Isotherm Data of Methane on zeolite 13X at 25, 50 ◦C measured by Simone Cavenati [19].

T= 25 ºC		**T= 5ºC**	
KPa P	mol/Kg q	KPa P	mol/Kg q
4.05	0.024	6.03	0.017
12.03	0.089	12.15	0.052
19.1	0.131	22	0.09
55.15	0.326	33.02	0.14
125	0.712	46.12	0.196
165	0.877	55.05	0.227
210	1.12	80.1	0.312
306	1.474	115	0.432

345	1.617	165	0.59
425	1.83	240	0.731
631	2.357	340	1.009
819	2.726	400	1.193
1070	3.06	510	1.423
1180	3.26	505	1.395
1410	3.53	635	1.653
1720	3.834	780	1.929
1890	3.991	865	2.077
2175	4.198	955	2.211
2610	4.506	1185	2.545
2985	4.75	1495	2.89
3365	4.987	1695	3.067
3560	5.103	1860	3.169
3745	5.191	2425	3.577
4260	5.469	2570	3.67
4725	5.719	3015	3.933
		3425	4.199
		3425	4.2
		3670	4.341
		4180	4.585
		4445	4.706
		4745	4.83

Table 3. 17: Henry's constant for the volumetric system compared to the ones in the literature.

Henry's constant (mol/Kg)	Temperature	Volumetric setup	Shivagi[31]	Ertan[8]	Park[18]	Kennedy[32]	Fillipe[33]
N2	25 °C	0.00377	3.297*10^-3	0.006	3.8*10^-3		
	50 °C	0.002015			1.973*10^-3		
	75 °C	0.00117				4.2744*10^-3	
CO2	25 °C	6.2928		2.62	0.7328		1.0285
	50 °C	0.2696			0.2696		
	75 °C	0.5668			6.776*10^-3		
CH4	25 °C	0.0066			6.776*10^-3		
	50 °C	0.0038			3.599*10^-3		
	75 °C	0.00239				4.906*10^-3	

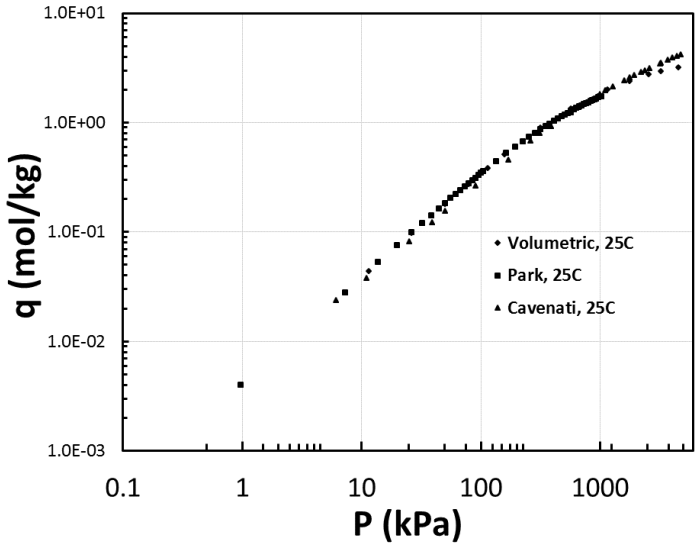

Figure 3. 10: comparison of the experimental adsorption isotherms of nitrogen on zeolite 13X at 25 °C against the ones found in the literature

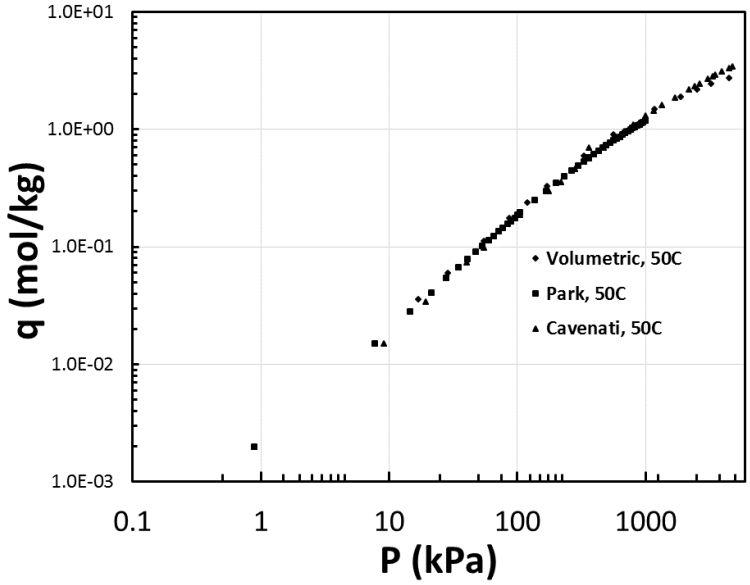

Figure 3. 11: comparison of the experimental adsorption isotherms of nitrogen on zeolite 13X at 50 °C against the ones found in the literature

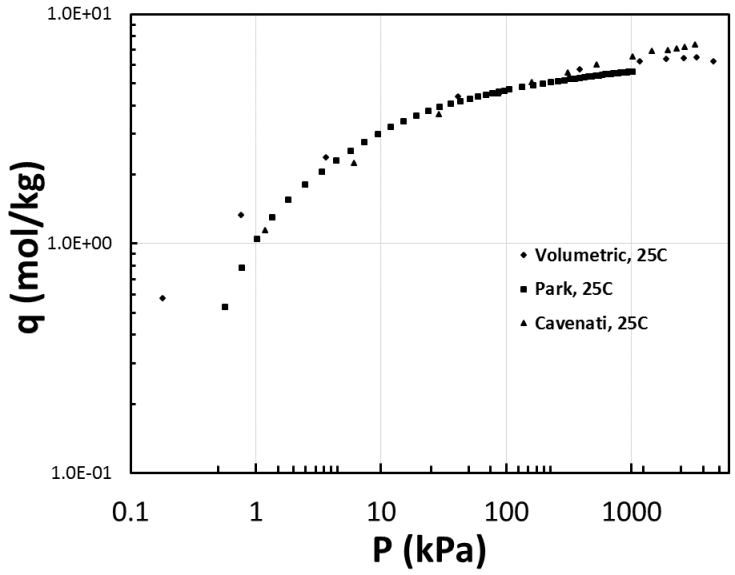

Figure 3. 12: comparison of the experimental adsorption isotherms of carbon dioxide on zeolite 13X at 25 ^{o}C against the ones found in the literature

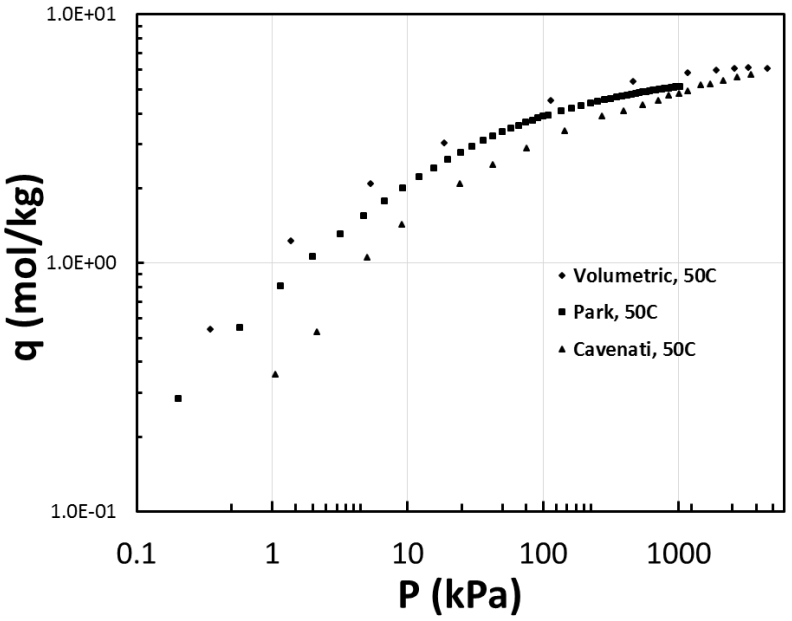

Figure 3. 13: comparison of the experimental adsorption isotherms of carbon dioxide on zeolite 13X at 50 ^{o}C against the ones found in the literature

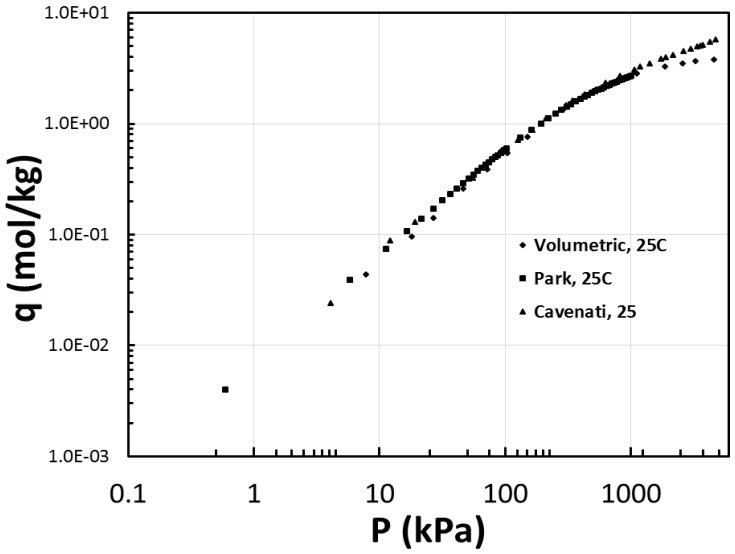

Figure 3. 14: comparison of the experimental adsorption isotherms of methane on zeolite 13X at 25°C against the ones found in the literature

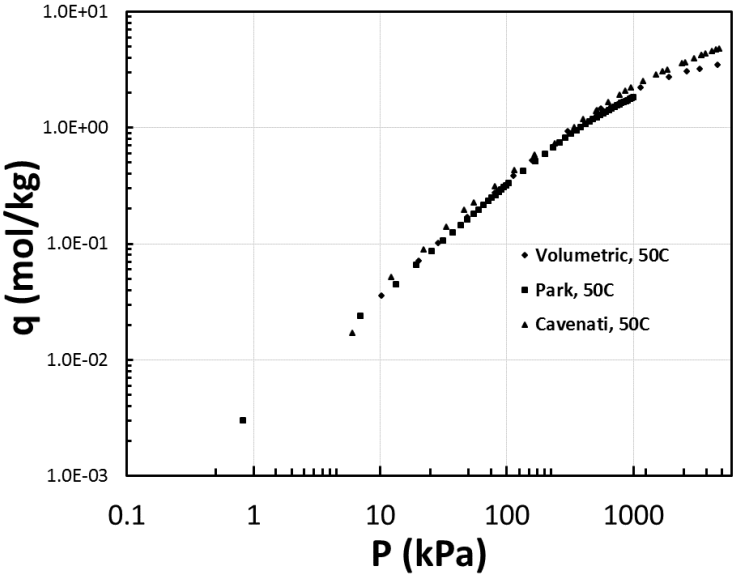

Figure 3. 15: comparison of the experimental adsorption isotherms of methane on zeolite 13X at 50 °C against the ones found in the

REFERENCES

[1] R.B. Jackson, A. Vengosh, T.H. Darrah, N.R. Warner, A. Down, R.J. Poreda, Increased stray gas abundance in a subset of drinking water wells near Marcellus shale gas extraction, (2013). doi:10.1073/pnas.1221635110/-/DCSupplemental.www.pnas.org/cgi/doi/10.1073/pnas.1221635110.

[2] R.D. Vidic, S.L. Brantley, J.M. Vandenbossche, D. Yoxtheimer, J.D. Abad, Impact of Shale Gas Development on Regional Water Quality Impact of Shale Gas Development, 340 (2013). doi:10.1126/science.1235009.

[3] T.W. Patzek, F. Male, M. Marder, Gas production in the Barnett Shale obeys a simple scaling theory, 110 (2013). doi:10.1073/pnas.1313380110.

[4] H. Rogers, Shale gas — the unfolding story, 27 (2011) 117–143. doi:10.1093/oxrep/grr004.

[5] J.M. Estrada, R. Bhamidimarri, Review article A review of the issues and treatment options for wastewater from shale gas extraction by hydraulic fracturing, 182 (2016) 292–303. doi:10.1016/j.fuel.2016.05.051.

[6] A.U.K. Perspective, G.P. Hammond, Á.O. Grady, D.E. Packham, Energy Technology Assessment of Shale Gas " Fracking ," Energy Procedia. 75 (2015) 2764–2771. doi:10.1016/j.egypro.2015.07.526.

[7] E. Methods, A. Isotherms, No Title, n.d.

[8] M.O.F. Science, CO_2 , N_2 and Ar Adsorption on Zeolites, (2004).

[9] O. Talu, Net Adsorption of Gas/Vapor Mixtures in Microporous Solids, (2013).

[10] S. Beutekamp, P. Harting, Experimental Determination and Analysis of High Pressure Adsorption Data of Pure Gases and Gas Mixtures, (2002) 255–269.

[11] R. V Siriwardane, M. Shen, E.P. Fisher, J.A. Poston, P.O. Box, W. Virginia, Adsorption of CO_2 on Molecular Sieves and Activated Carbon, (2001) 279–284.

[12] S. Himeno, T. Komatsu, S. Fujita, High-Pressure Adsorption Equilibria of Methane and Carbon Dioxide on Several Activated Carbons, (2005) 369–376.

[13] D.P. Vargas, L. Giraldo, Carbon dioxide and methane adsorption at high pressure on activated carbon materials, (2013) 1075–1082. doi:10.1007/s10450-013-9532-5.

[14] E.G.J.B.P.C.O. Ania, A.G.J.M.V.B.R. Krishna, D.D.S. Calero, A computational

study of CO_2 , N_2 , and CH_4 adsorption in zeolites, (2007) 469–476. doi:10.1007/s10450-007-9039-z.

[15] J. Ma, C. Si, Y. Li, R. Li, CO_2 adsorption on zeolite X / activated carbon composites, (2012) 503–510. doi:10.1007/s10450-012-9440-0.

[16] L.H.L.C.G. De Weireld, Determination of absolute gas adsorption isotherms : simple method based on the potential theory for buoyancy effect correction of pure gas and gas mixtures adsorption, (2014) 397–408. doi:10.1007/s10450-013-9579-3.

[17] C. Gomes, Experimental High-Throughput Adsorption Unit for Multi-Evaluation of Adsorbents for Gas Capture , Storage and Separation Applications, (2014).

[18] M. Co, Y. Park, Y. Ju, D. Park, C. Lee, Adsorption equilibria and kinetics of six pure gases on pelletized zeolite, Chem. Eng. J. 292 (2016) 348–365. doi:10.1016/j.cej.2016.02.046.

[19] S. Cavenati, C.A. Grande, E. Rodrigues, Adsorption Equilibrium of Methane , Carbon Dioxide , and Nitrogen on Zeolite 13X at High Pressures, (2004) 1095–1101.

[20] Y. Takamura, S. Narita, J. Aoki, S. Uchidal, Process for Improvement of CO , Recovery System from Flue Gas, 79 (2001) 812–816.

[21] A.M. Martini, L.M. Walter, T.C.W. Ku, J.M. Budai, J.C. Mcintosh, M. Schoell, Microbial production and modification of gases in sedimentary basins : A geochemical case study from a Devonian shale gas play , Michigan basin, 8 (2003) 1355–1375. doi:10.1306/031903200184.

[22] J. Dai, Y. Ni, D. Gong, Z. Feng, D. Liu, W. Peng, W. Han, Geochemical characteristics of gases from the largest tight sand gas fi eld (Sulige) and shale gas fi eld (Fuling) in China, Mar. Pet. Geol. 79 (2017) 426–438. doi:10.1016/j.marpetgeo.2016.10.021.

[23] G. Etiope, A. Drobniak, A. Schimmelmann, Natural seepage of shale gas and the origin of " eternal fl ames " in the Northern Appalachian Basin , USA, Mar. Pet. Geol. 43 (2013) 178–186. doi:10.1016/j.marpetgeo.2013.02.009.

[24] J. Dai, C. Zou, S. Liao, D. Dong, Y. Ni, J. Huang, W. Wu, Organic Geochemistry Geochemistry of the extremely high thermal maturity Longmaxi shale gas , southern Sichuan Basin, Org. Geochem. 74 (2014) 3–12. doi:10.1016/j.orggeochem.2014.01.018.

[25] J.A. Ritter, S.J. Bhadra, A.D. Ebner, On the Use of the Dual-Process Langmuir Model for Correlating Unary Equilibria and Predicting Mixed-Gas Adsorption Equilibria, (2011) 4700–4712.

[26] A. Chakraborty, B.B. Saha, K. Srinivasan, K.C. Ng, Theory and experimental validation on isosteric heat of adsorption for an adsorbent + adsorbate system †, 37 (2008) 109–117.

[27] H. Pan, J.A. Ritter, P.B. Balbuena, Functional Theory, 5885 (1998) 1159–1166.

[28] Manuscript-13X USC-Nima, (n.d.). To be puplished

[29] R.T. Yang, FUNDAMENTALS AND APPLICATIONS, n.d.

[30] L. Bonneviot, S. Kaliaguine, ZEOLITES A REFINED TOOL FOR DESINGING CATALYTIC SITES, n.d.

[31] A.L. Myers, Gas Separation by Zeolites, (2003).

[32] D.A. Kennedy, M. Mujcin, E. Trudeau, F.H. Tezel, Pure and Binary Adsorption Equilibria of Methane and Nitrogen on Activated Carbons , Desiccants , and Zeolites at Di ff erent Pressures, (2016). doi:10.1021/acs.jced.6b00245.

[33] F.V.S. Lopes, C.A. Grande, A.M. Ribeiro, J.M. Loureiro, O. Evaggelos, V. Nikolakis, A.E. Rodrigues, F.V.S. Lopes, C.A. Grande, A.M. Ribeiro, J.M. Loureiro, O. Evaggelos, V. Nikolakis, A.E. Rodrigues, Adsorption of H_2 , CO_2 , CH_4 , CO , N_2 and H_2O in Activated Carbon and Zeolite for Hydrogen Production, 6395 (2009). doi:10.1080/01496390902729130.

[33] 738__90f7b57.pdf, (n.d.).